Supporting Information

for

Ferrocenyl-Functionalized Phenothiazine Conjugates: Structure-Property Relationship and Electrochemical Energy Storage Studies

Deeksha Gupta,[a,b] Nikhil Ji Tiwari,[a] Vivak Kandpal,[a] Prabal Pratap Singh,[b] and Rajneesh Misra[*,a]*

* Corresponding Author

D. Gupta, N. J. Tiwari, V. Kandpal, R. Misra

[a]Department of Chemistry, Indian Institute of Technology Indore, Indore- 453552, India.

E-mail: rajneeshmisra@iiti.ac.in

D. Gupta, P. P. Singh

[b]Department of Chemistry, GLA University17 km Stone, NH-2 Delhi-Mathura Highway, Chaumuhan, Mathura, Uttar Pradesh, India

Experimental Details

Chemicals were used as received unless otherwise indicated. All the oxygen- or moisture-sensitive reactions were carried out under an argon atmosphere, and the reflux reactions were performed in an oil bath. ^{1}H NMR (500 MHz) spectra were recorded on a Bruker 500 MHz FT-NMR spectrometer at room temperature. Chemical shifts are reported in delta (δ) units, expressed in parts per million (ppm) downfield from tetramethyl silane (TMS) using the deuterated solvents as an internal standard {$CDCl_3$, 7.26 ppm; DMSO-d_6, 2.50 ppm}. The Multiplicities are given as s (singlet), d (doublet), t (triplet) and m (multiplet) and the coupling constants, J, are given in hertz. ^{13}C NMR (126 MHz) on a Bruker 500 MHz FT-NMR spectrometer at room temperature. Chemical shifts are reported in delta (δ) un its, expressed in parts per million (ppm) downfield from TMS using the solvent as internal standard {$CDCl_3$, 77.16 ppm; DMSO-d_6, 39.52 ppm}. Thermogravimetric analysis was performed on the Mettler Toledo thermal analysis system. UV-visible absorption spectra of all compounds were recorded on a PerkinElmer Lambda 35 instrument in the DCM solution. All the measurements were carried out at 25 °C. HRMS were recorded on a Bruker-Daltonics micrOTOF-Q II mass spectrometer. The cyclic and differential pulse voltammograms (CVs and DPVs) were recorded on a PalmSens 4 electrochemical analyzer in the DCM solvent using glassy carbon as a working electrode, Pt wire as the counter electrode, and Ag/AgCl as the reference electrode. The scan rate was 100 mV s^{-1} for CV. A solution of tetrabutylammonium hexafluorophosphate ($[N(C_4H_9)_4]^+$ $[PF_6]^-$) in DCM (0.1 M) was used as the supporting electrolyte. Spectroelectrochemical measurements were done using a commercially available platinum honeycomb working electrode on a ceramic support in a narrow optical path quartz cuvette using a miniature Ag/AgCl gel electrode as a reference electrode. The potential was controlled and switched with a potentiostate. The resulting spectroscopic changes were measured with ALS SEC2020 spectrometer system. DFT calculations were performed using the B3LYP/6-31G(d,p) (B3LYP functional with the 6-31G(d,p) basis set) for C, H, S, O, and N atoms, and the LanL2DZ basis set for the Fe atom.[1] The working electrodes **1/GF, 2/GF** and **3/GF** were fabricated by preparing a uniform slurry composed of **1**, **2** and **3** (active material), carbon black (conductive additive) and poly(vinylidene fluoride) (PVDF) binder in a weight proportion of 70:20:10. The mixture was carefully grinded to achieve a fine, homogeneous blend and subsequently dispersed in N-methyl-2-pyrrolidone (NMP) as the solvent. The resulting slurry was uniformly applied onto a graphite foil (GF) substrate with a surface area of 1 × 1 cm^2. The coated electrode was then

placed in a hot-air oven at 80 °C and dried for 12 h to ensure consistent film formation and complete solvent evaporation. The final electrode contained approximately 1.8 (± 0.2) mg of the active material forming a stable and well-adhered coating suitable for electrochemical studies. The CCDC number 2433585 contains the supplementary crystallographic data for **1**.

FTIR spectroscopic analysis:

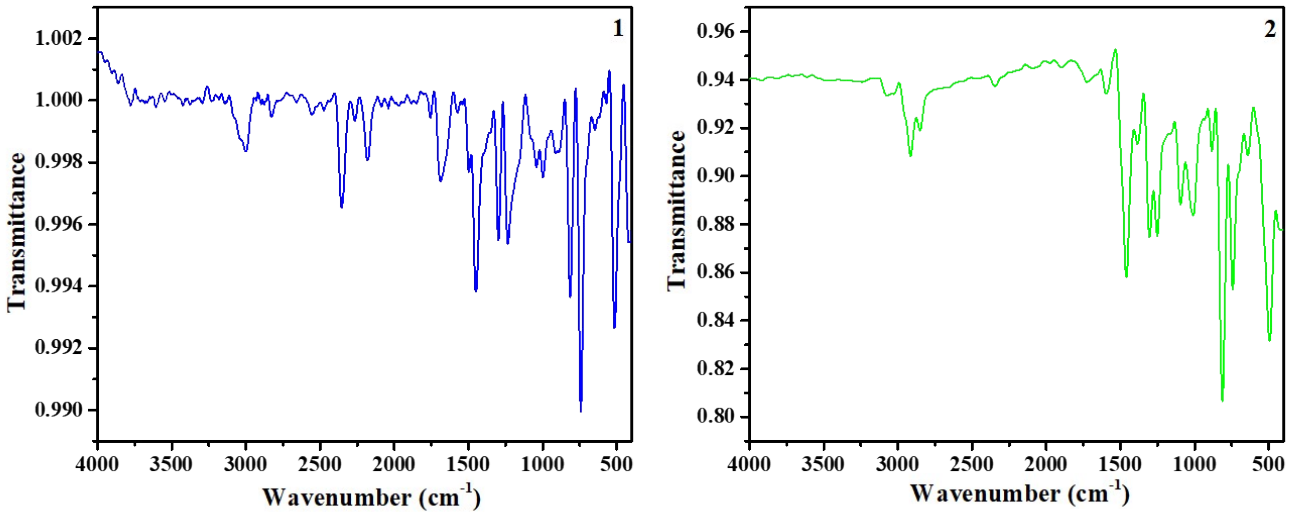

Fig. S1. FTIR spectra of ferrocenyl functionalized phenothiazine conjugates **1–2**.

(a)

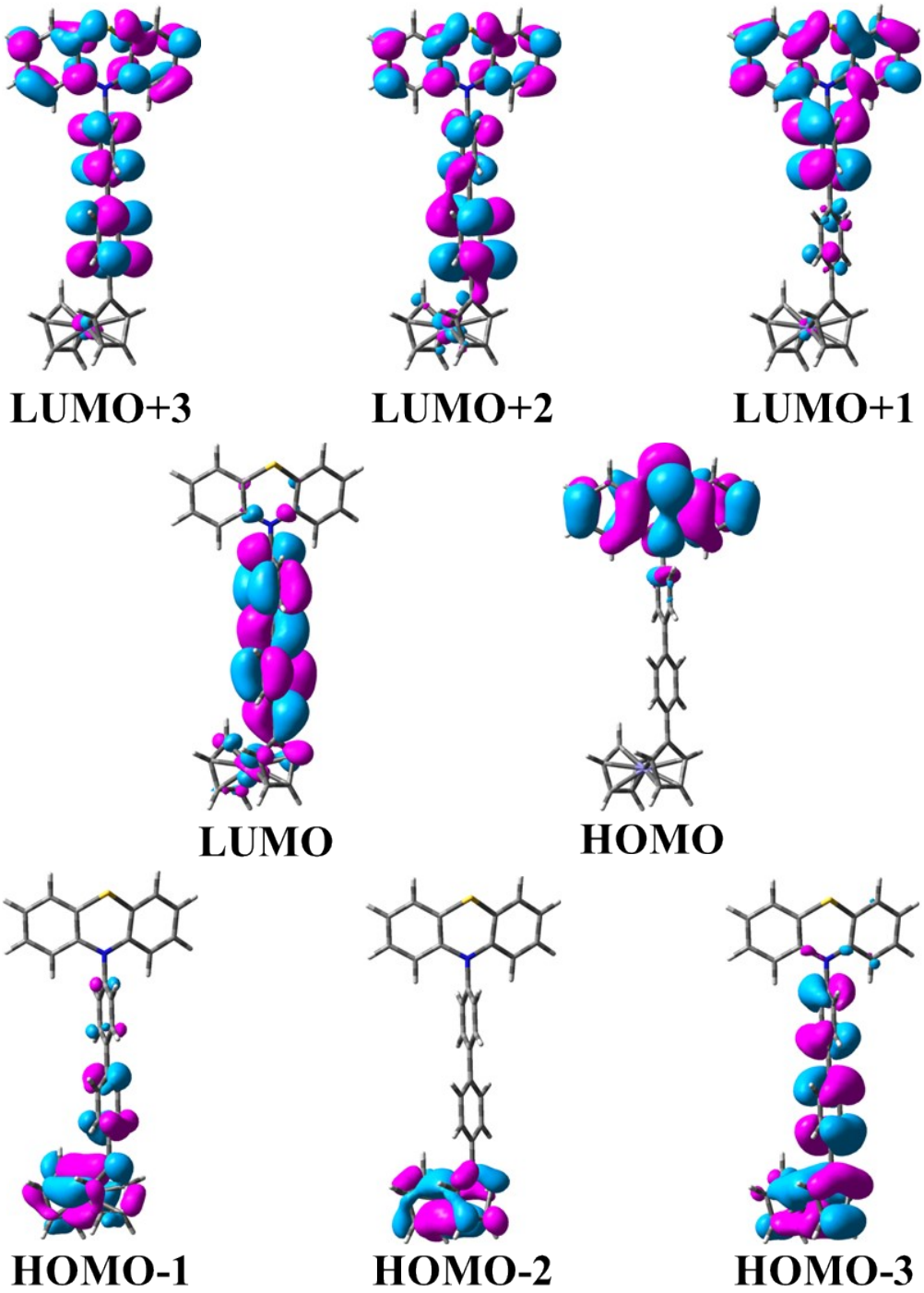

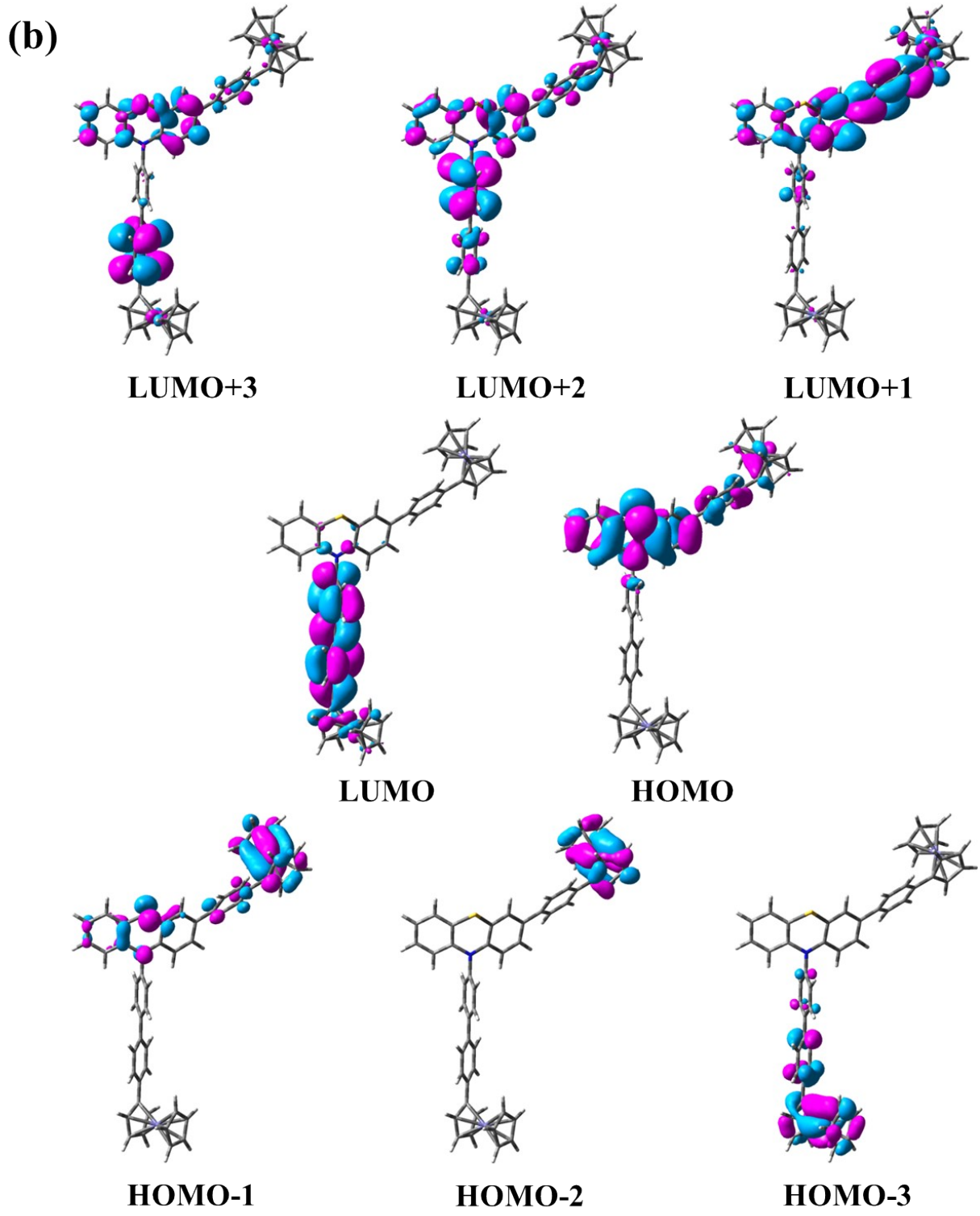

Fig. S2. The molecular orbitals of (a) **1** and (b) **2** are estimated from DFT calculation.

Table S1: Energy levels and their differences in a molecular system.

Compounds	HOMO-3	HOMO-2	HOMO-1	HOMO	LUMO	LUMO+1	LUMO+2	LUMO+3
1	-5.95	-5.38	-5.30	-4.92	-1.19	-0.54	-0.28	-0.19
2	-5.30	-5.22	-5.18	-4.84	-1.23	-0.88	-0.53	-0.24
3	-5.23	-5.20	-5.15	-4.78	-1.23	-1.01	-0.72	-0.54

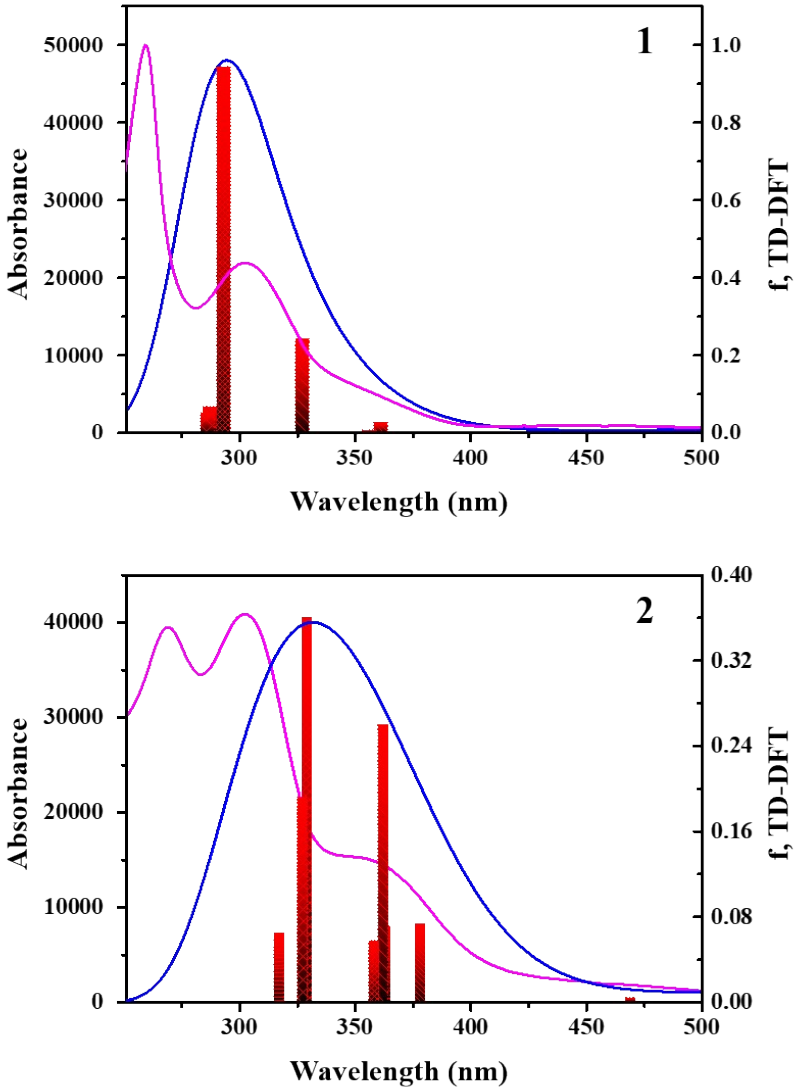

Fig. S3. TDDFT-predicted (blue) and experimental (pink) UV-Vis absorption spectra of **1** and **2** in DCM.

Electrochemical performance of ferrocenyl conjugate 2/GF

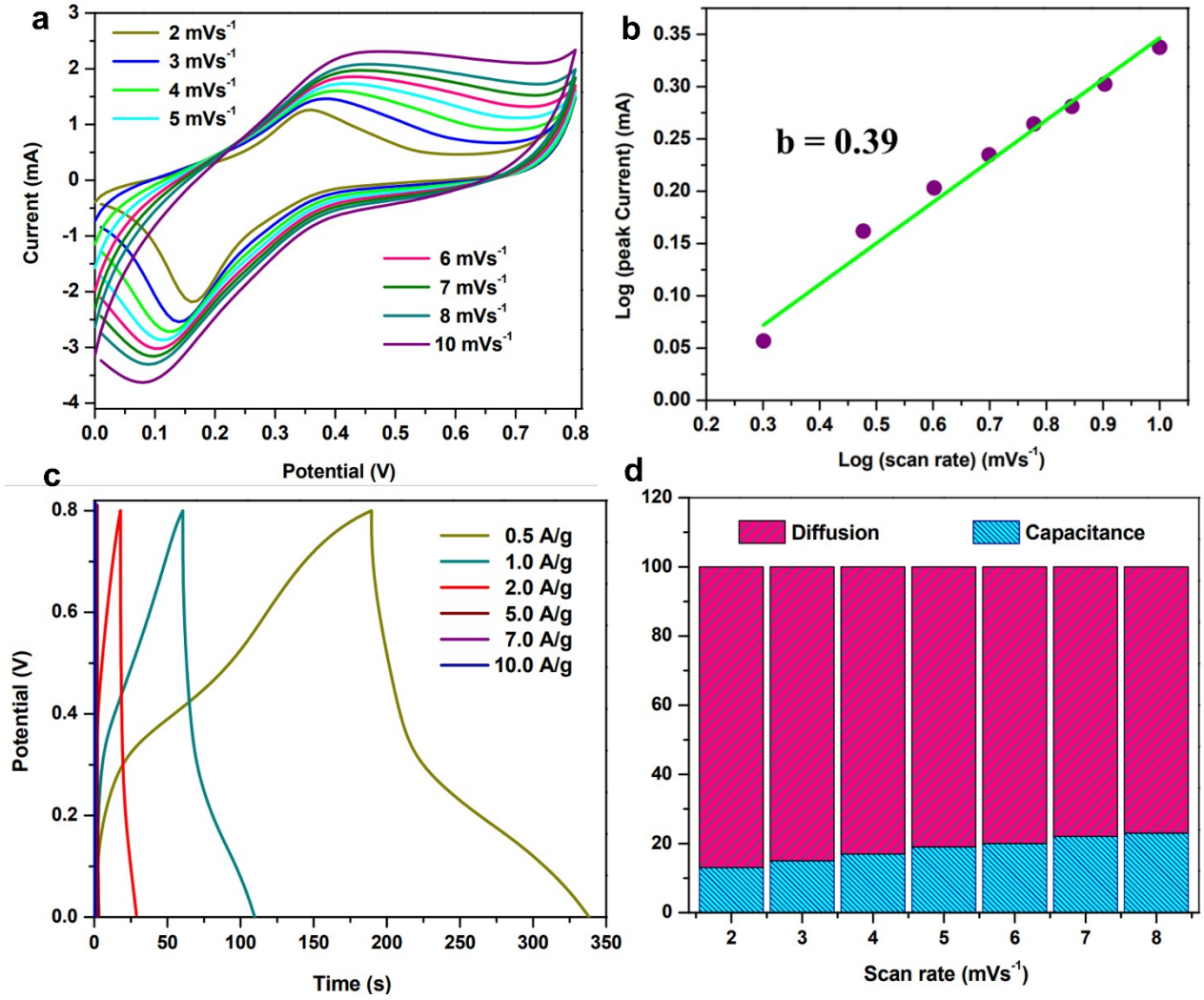

Fig. S4. Electrochemical performance of ferrocenyl conjugate **2/GF** in three-electrode setup. (a) CV curves; (b) linear fitting plot between log(*i*) and log(*v*); (c) GCD curves; (d) ratios of capacitive and diffusion contribution at different scan rates.

Electrochemical performance of ferrocenyl conjugate 3/GF

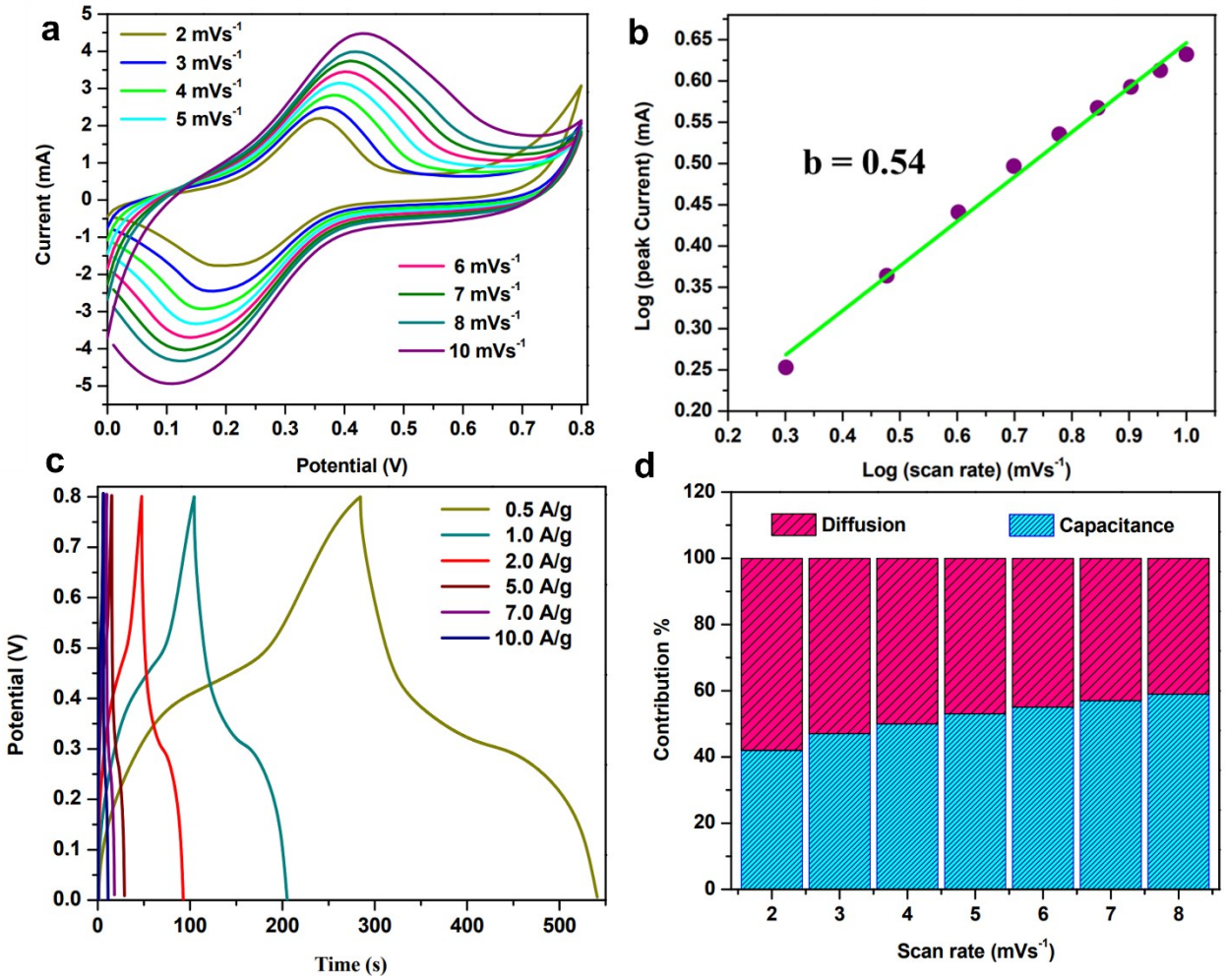

Fig. **S5**. Electrochemical performance of ferrocenyl conjugate **3/GF** in three-electrode setup. (a) CV curves; (b) linear fitting plot between log(*i*) and log(*v*); (c) GCD curves; (d) ratios of capacitive and diffusion contribution at different scan rates.

Cyclic stability for 2/GF and 3/GF

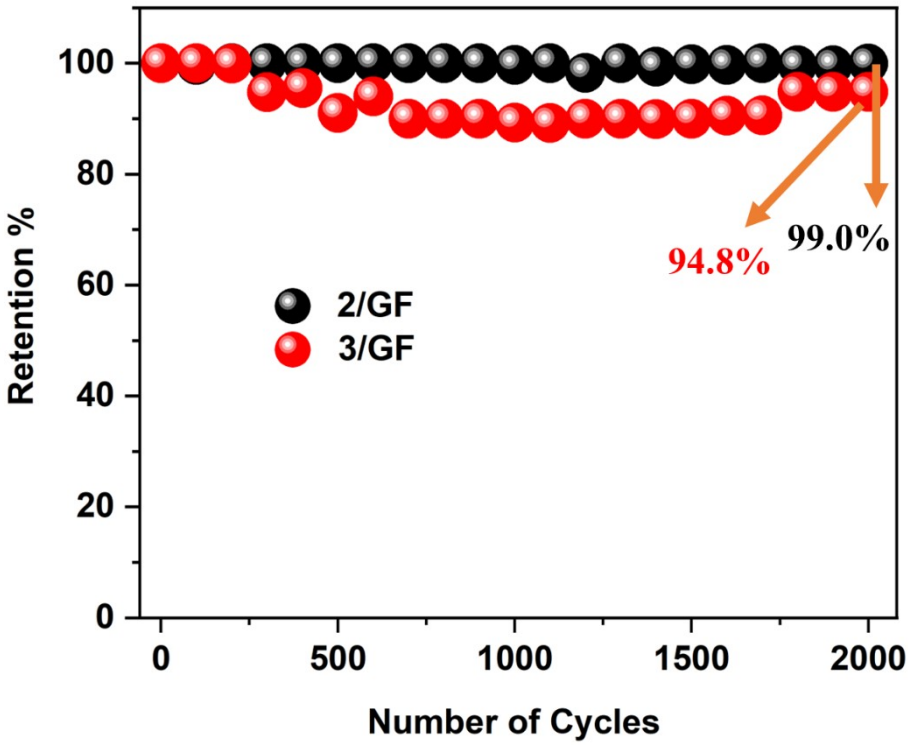

Fig. S6. Cyclic stability for **2/GF** and **3/GF** at 10.0 A g^{-1} for 2000 cycles.

Table S2. Discharge specific capacitance of ferrocenyl conjugates **1–3** drop casted on the graphite foil (GF).

Current Density (Ag^{-1})	Discharge Specific Capacitance (Fg^{-1})		
	1/GF	2/GF	3/GF
0.5	80.0	93.3	160.8
1.0	72.5	61.9	125.7
2.0	60.5	28.0	112.8
5.0	38.1	7.1	85.4
7.0	29.0	3.6	75.6
10.0	17.9	2.0	63.3

Table S3. Comparison of discharge specific capacitance of **1/GF and 3/GF** with different electrode materials reported in the literature.

S. No.	Reference	Electrode Material	Electrolyte	Voltage (V)	Current density ($A\ g^{-1}$)	*C*sp GCD ($F\ g^{-1}$)
1.	**This work**	**3/GF** and **1/GF**	**1.0 M H_2SO_4**	**0.0 to 0.8**	**0.5**	**160.8** and **80.0**
2.	103	PTZ-Ph-PTZ/GF	1.0 M H_2SO_4	-0.2 to 0.8	0.5	286.11
3.	104	PTZ-AQ-PTZ/r-GO	1.0 M H_2SO_4	-0.2 to 0.8	0.5	181.85
4.	78	AQ-ImPTZ-Im-AQ/GF and PTZ-Im-AQ/GF	1.0 M H_2SO_4	-0.4 to 0.8	0.5	243.15 and 175.26
5.	105	PTZ/r-GO aerogel (P8G1)	5.0 M KOH	-1.0 to 0.0	0.5	235.5
6.	106	GO-FBF1/ PPy and GO-FBF2/PPy nano-composites	1.0 M Na_2SO_4	-0.2 to 1.0	1.0	229.43 and 269.57 *(in mA hg^{-1})**
7.	107	Py-BZFC-CMP-800 and Py-PHFC-CMP-800	6.0 M KOH	-1.0 to 0.0	0.5	182 and 324
8.	108	MOF $[Zn_9(Cei)_6(Bimb)_9]_n$	1.0 M ACN	0.0 to 1.0	1.0	33

Single Crystal x-ray Diffraction Studies:

Single crystal x-ray structural studies of **1** were performed on a CCD Agilent Technologies (Oxford Diffraction) SUPER NOVA diffractometer. Data were collected at 293(2) K using graphite-monochromated Mo Kα radiation (λ_α = 0.71073 Å). Unit cell determination, data collection and reduction, and empirical absorption correction were performed using the CrysAlisPro program. The data were collected by the standard 'phi-omega scan techniques, and were scaled and reduced using CrysAlisPro RED software. The Olex 2–1.5 program[2] was used as the graphical interface. The structures were solved by direct methods using SHELXT,[3] which revealed the positions of all not disordered non-hydrogen atoms. The structure model was refined using full matrix least squares minimization on F^2 using ShelXL[4] within Olex2 for a graphical interface. The positions of all the atoms were obtained by direct methods. All non-hydrogen atoms were refined anisotropically. The remaining hydrogen atoms were placed in geometrically constrained positions, and refined with isotropic temperature factors, generally 1.2U_{eq} of their parent atoms. The crystal and refinement data are summarized in Table S1. The CCDC number **2433585** contains the supplementary crystallographic data for **1**. These data can be obtained free of charge via www.ccdc.cam.ac.uk/conts/retrieving.html (or from the Cambridge Crystallographic Data Centre, 12 union Road, Cambridge CB21 EZ, UK; Fax: (+44) 1223-336 033; or deposit@ccdc.cam.ac.uk).

Single Crystal x-ray Analysis

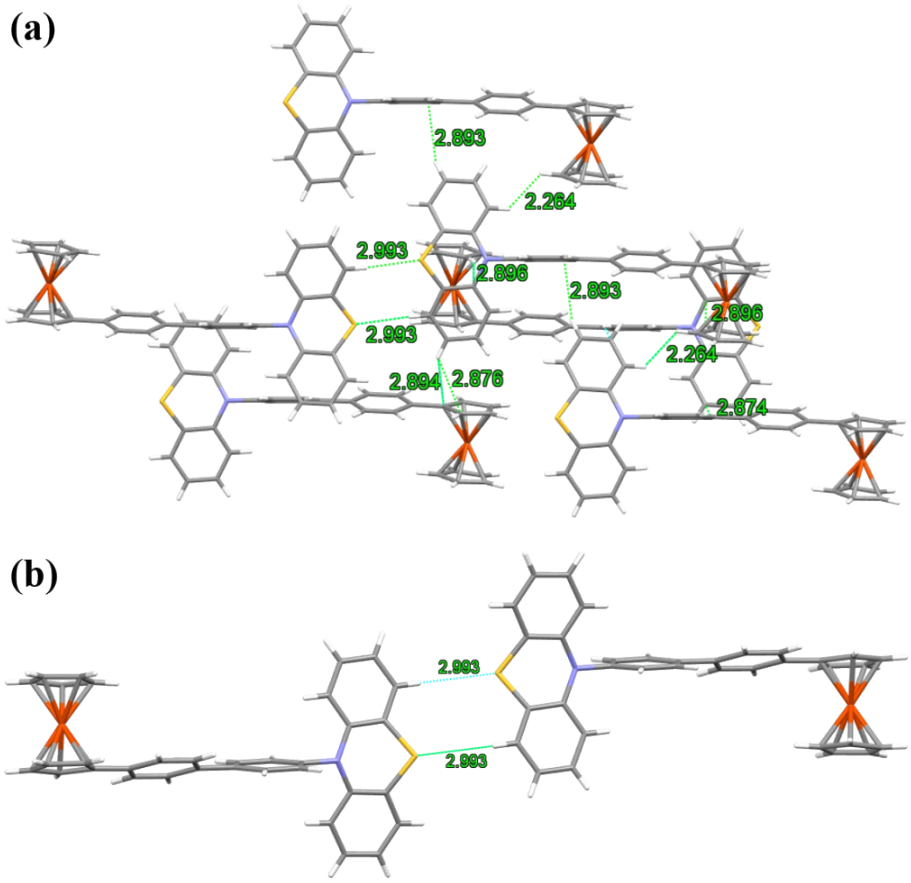

Fig. S7. Crystal packing diagrams of ferrocenyl-functionalized phenothiazine derivatives **1**. (a) C–H···π interactions in **1** (b) S–H hydrogen bonding interactions between the packing diagram of **1**.

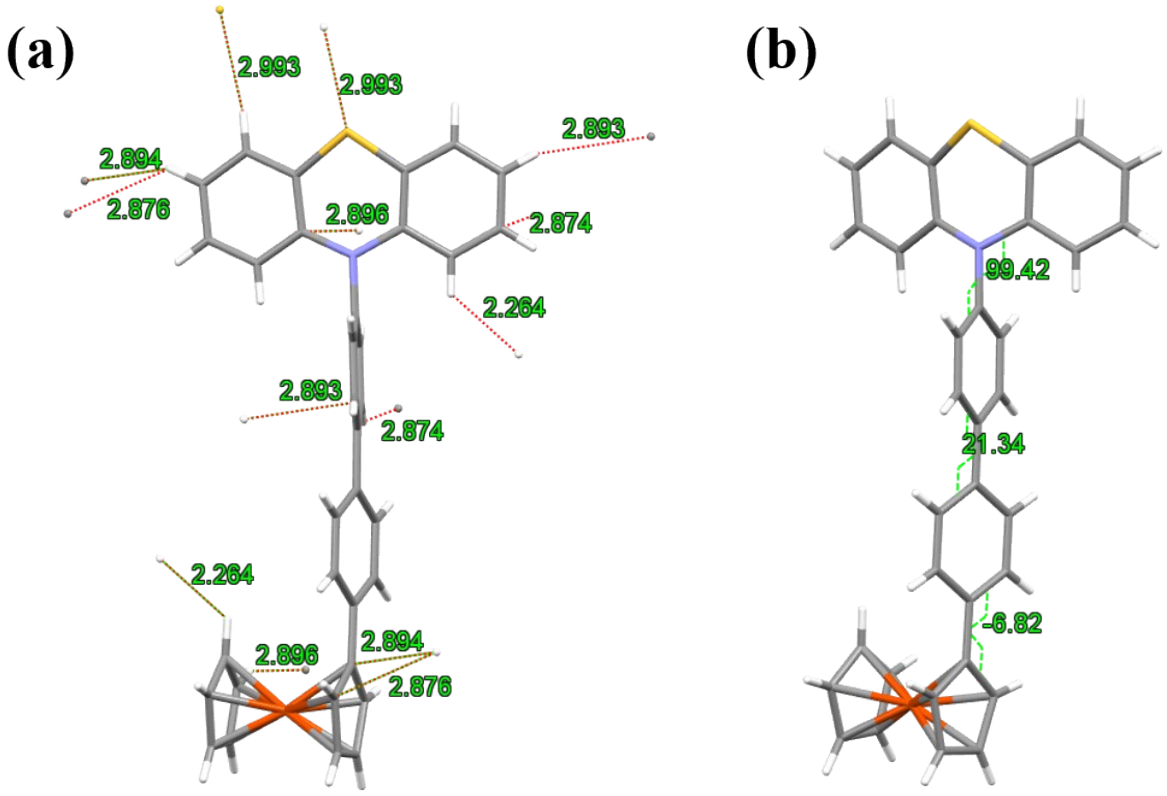

Fig. S8. (a) All the different intermolecular interactions between the molecules of **1**. (b) Torsion angles between the key atoms of phenothiazine, phenyl, and ferrocenyl unit of the **1**.

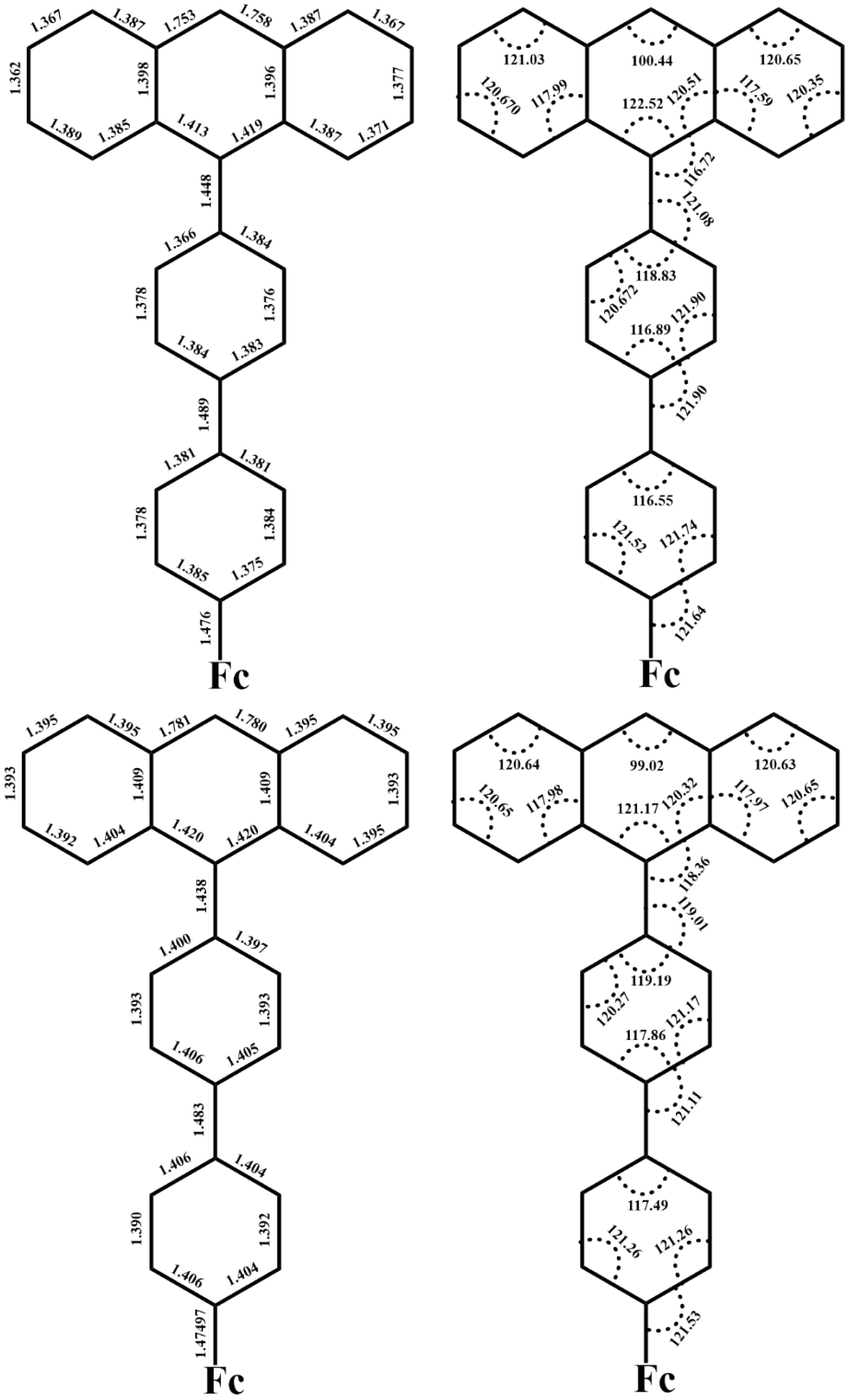

Fig. S9. Comparable study of bond lengths and bond angles of the crystal structures (above) and DFT optimized structures (below) of the ferrocenyl functionalized phenothiazine derivatives **1**.

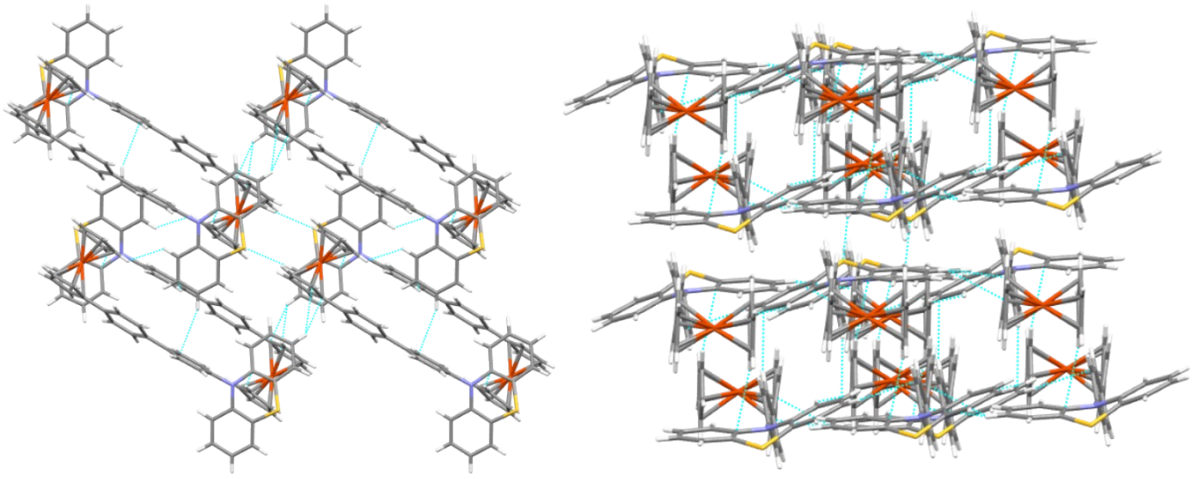

Fig. S10. Crystal packing diagrams of ferrocenyl-functionalized phenothiazine conjugates **1**.

RM-NJT-DG-4B.001.001.1r.esp

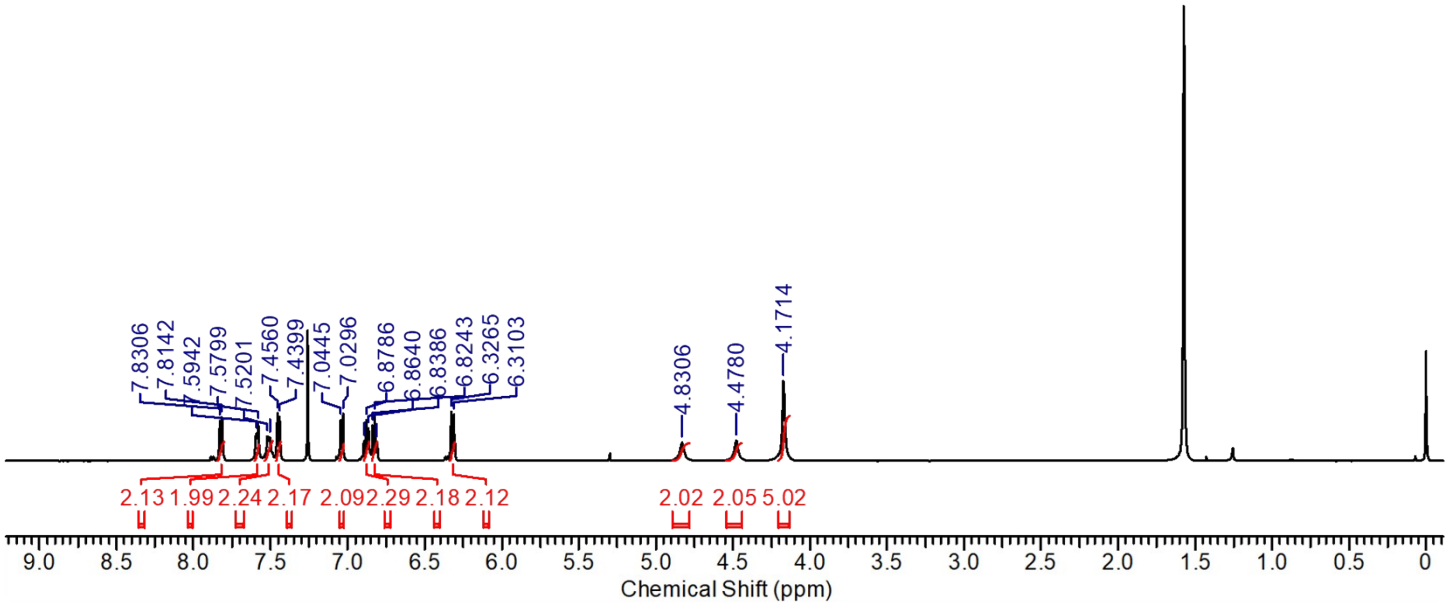

Fig. S11. ^{1}H NMR of **1**.

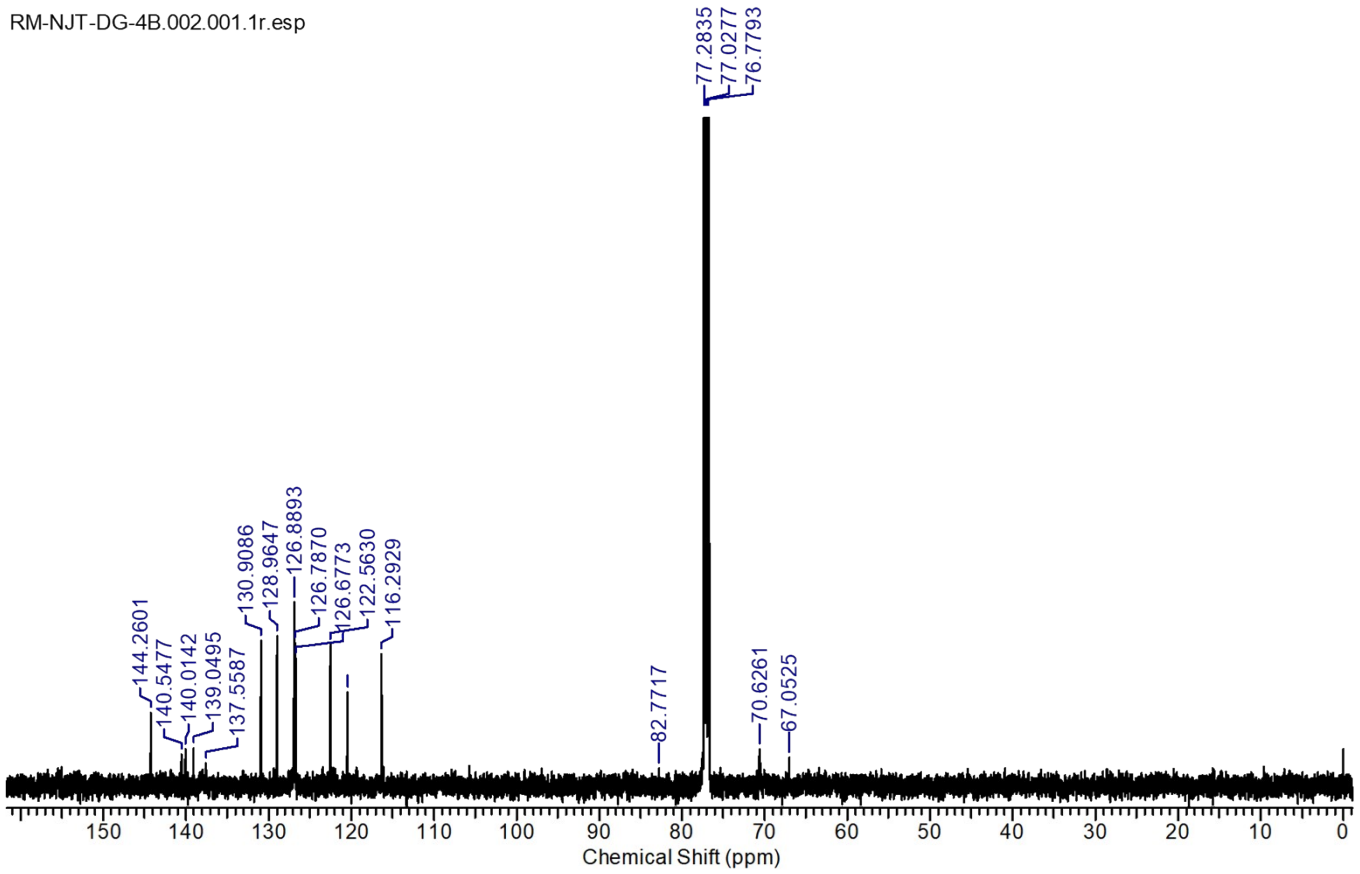

Fig. S12. ^{13}C NMR of **1**.

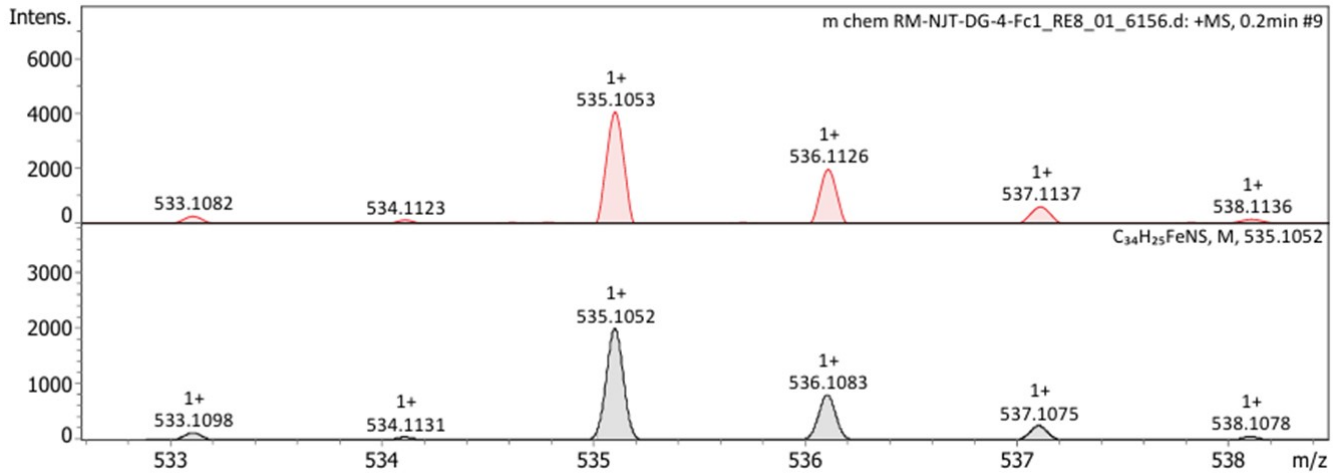

Fig. S13. HRMS of **1**.

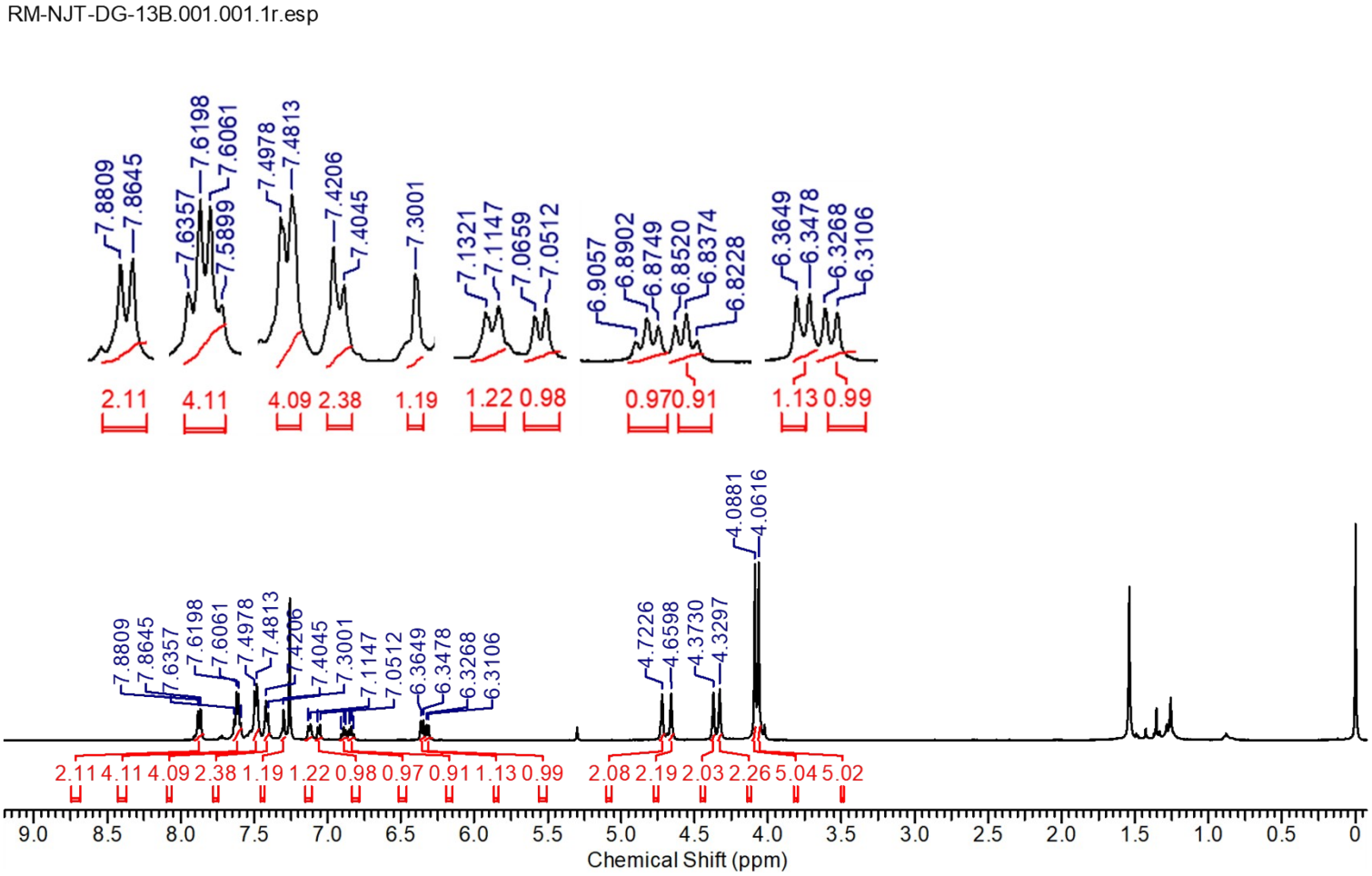

Fig. S14. ^{1}H NMR of **2**.

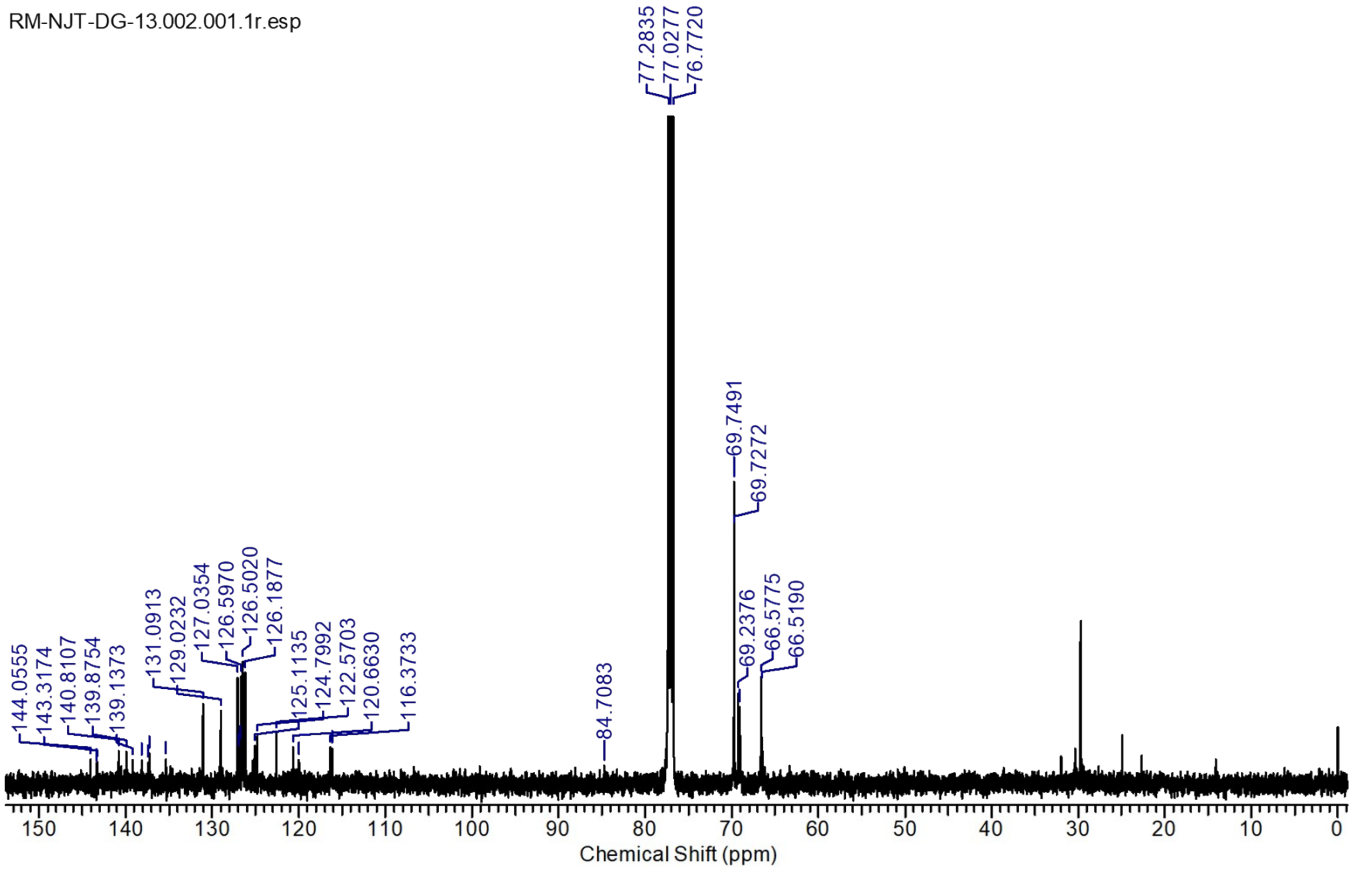

Fig. S15. ^{13}C NMR of **2**.

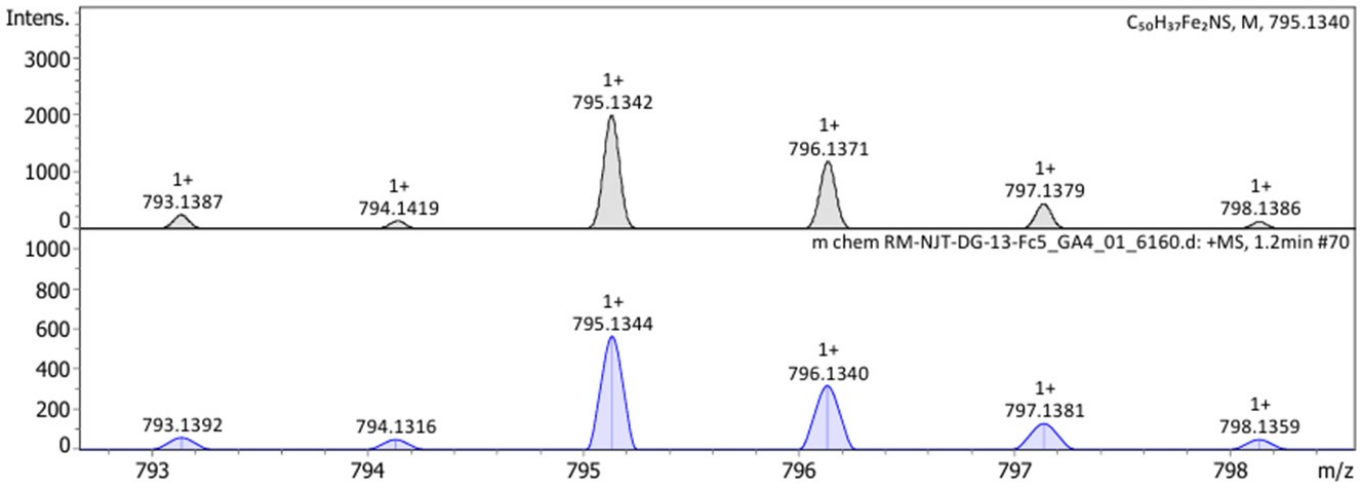

Fig. S16. HRMS of **2**.

References:

1. Gaussian 09, Revision 09 W, M. J. Frisch, G. W. Trucks, H. B. Schlegel, G. E. Scuseria, M. A. Robb, J. R. Cheeseman, G. Scalmani, V. Barone, B. Mennucci, G. A. Petersson, H. Nakatsuji, M. Caricato, X. Li, H. P. Hratchian, A. F. Izmaylov, J. Bloino, G. Zheng, J. L. Sonnenberg, M. Hada, M. Ehara, K. Toyota, R. Fukuda, J. Hasegawa, M. Ishida, T. Nakajima, Y. Honda, O. Kitao, H. Nakai, T. Vreven, J. A. Montgomery, Jr., J. E. Peralta, F. Ogliaro, M. Bearpark, J. J. Heyd, E. Brothers, K. N. Kudin, V. N. Staroverov, R. Kobayashi, J. Normand, K. Raghavachari, A. Rendell, J. C. Burant, S. S. Iyengar, J. Tomasi, M. Cossi, N. Rega, J. M. Millam, M. Klene, J. E. Knox, J. B. Cross, V. Bakken, C. Adamo, J. Jaramillo, R. Gomperts, R. E. Stratmann, O. Yazyev, A. J. Austin, R. Cammi, C. Pomelli, J. W. Ochterski, R. L. Martin, K. Morokuma, V. G. Zakrzewski, G. A. Voth, P. Salvador, J. J. Dannenberg, S. Dapprich, A. D. Daniels, Farkas, J. B. Foresman, J. V. Ortiz, J. Cioslowski, D. J. Fox, Gaussian, Inc. Wallingford CT, 2009.
2. O. V. Dolomanov, L. J. Bourhis, R. J. Gildea, J. A. K. Howard, H. Pusch-mann, *J. Appl. Crystallogr.* 2009, **42**, 339–341.
3. G. M. Sheldrick, *Acta Crystallogr.* 2015, **71**, 3–8.
4. G. M. Sheldrick, *Acta Crystallogr.* 2008, **64**, 112–122.